
Article:
Wang, G., Wei, H.-L. orcid.org/0000-0002-4704-7346 and Liu, Z.-H. (2024) An intelligent state evaluation and maintenance arrangement system for wind turbines based on digital twin. Academia Engineering, 1 (4). ISSN 2994-7065

https://doi.org/10.20935/acadeng7391

ACADEMIA ENGINEERING

Research Article
Published: 2024-10-28
https://doi.org/10.20935/AcadEng7391

An intelligent state evaluation and maintenance arrangement system for wind turbines based on digital twin

Guoliang Wang[1], Hua-Liang Wei[1,*], Zhao-Hua Liu[2]

Academic Editor: Khaled Sallam

Abstract

Wind power is an important green and sustainable source of power generation. However, the construction of wind farms does not only need a large amount of initial investment but also highly expensive maintenance cost for their operations during power generation. Therefore, accurately assessing the state of wind turbines and effectively scheduling maintenance to keep them in good operating condition have become crucially important to ensure efficient power generation. Digital twin, as a data-driven digital concept or technology, can be used to effectively address wind power maintenance issues, especially wind turbine state evaluation problem. This article proposes a novel intelligent state evaluation and maintenance arrangement (iSEMA) system based on digital twin, which can accurately evaluate the state of wind turbines, detect faults in the early stage, and provide useful information or warnings to operators and help them to efficiently arrange maintenance tasks. In addition, this article introduces the concept of sub-healthy state of wind turbines, which is very useful for designing the iSEMA system. Experimental results demonstrate that the proposed system can assess the state of wind turbines accurately and provide timely feedback.

Keywords: *wind turbine, state evaluation, maintenance arrangement, long short-term memory, digital twin*

Citation: Wang G, Wei HL, Liu ZH. An intelligent state evaluation and maintenance arrangement system for wind turbines based on digital twin. *Academia Engineering* 2024;1. https://doi.org/10.20935/AcadEng7391

1. Introduction

To reduce the impacts of global warming and protect Earth's environment, people now are more inclined to choose clean energies instead of traditional fossil fuels. Wind energy as one of the cleanest energies now account for a quarter of all kinds of power generation [1]. Due to the high level of noise, wind turbines (WTs) are typically built in remote locations away from cities, such as mountains or offshore areas. Therefore, maintenance tasks are essential for the proper operation of WTs. According to [2], the cost of maintenance after failure is nearly three times the cost of regular maintenance. If the faults can be detected and addressed early, it will significantly reduce maintenance costs. Thus, it is crucial to accurately assess the condition of WTs and schedule maintenance work effectively.

Digital twin (DT) was first proposed by Michael Grieves [3] in 2003 to better manage the lifecycle of physical products. After that, Michael Grieves and many other researchers have expanded the definition of DT that can be typically described as an integrated entity of a physical product, a virtual description of that product, and the data communication between them [4]. In recent years, DT has been applied in various fields and promotes positive developments in these areas. In one study [5], the applications of DT in energy storage were reviewed, demonstrating the positive developments with DT in this field and discussing the challenges of DT. In the field of manufacturing, DT can provide a real-time response of the manufacture system and increase flexibility [6]. In another work [7], the possibilities and challenges of DT for the construction of smart cities were comprehensively reviewed. In addition to the aforementioned fields, DTs have also been employed in WTs to ensure their stable operation more effectively. A real-time planetary gear fault diagnosis method was proposed by Wang et al. [8] by combining the atom search optimization-support vector machine and DT which can significantly improve the operation of WTs. Kim et al. [9] utilize various environmental information to design a predictive model for offshore WT power generation based on DT. The proposed system enables an accurate representation of the offshore WT power generation and proposes contributions to the safety of the power system.

To characterize the dynamic behaviors of WTs, mathematical equations or models based on First Principles can be used to construct virtual representations of physical entities. For example, in the work by Kim et al. [9], five equations are used to describe the various behaviors of the WT system, while Xie et al. [10] used around 10 equations to describe bearings. In both studies [9] and [10], the First Principles models are used to build a DT which can significantly facilitate the study of the original physical systems (e.g., to generate data via numerical simulations by considering a variety of environmental conditions). It may not be highly

[1]Department of Automatic Control and Systems Engineering, University of Sheffield, Sheffield, South Yorkshire S1 3JD, UK.
[2]School of Information and Electrical Engineering, Hunan University of Science and Technology, Xiangtan, Hunan Province 411201, China.
*email: w.hualiang@sheffield.ac.uk

difficult to obtain mathematical models to describe the behaviors of WTs for some specific tasks, but for many real application scenarios where WTs are installed in harsh environments with severe climatic conditions, it may not be straightforward to build reliable mathematical models. As an attractive alternative, data-driven modeling techniques, such as system identification [11, 12], reduced-order models [13], joint load-response estimation based on unified linear input and state modeling methods [14], and machine learning methods [15–17], provide a powerful tool which can learn and extract some useful information from data without the need of prior knowledge of the original physical systems; the learned information or extracted features can usually be used to perform fault detection and diagnosis tasks.

This work proposes a novel intelligent state evaluation and maintenance arrangement (iSEMA) system of WTs by innovatively combining deep learning and DT technology, where long short-term memory (LSTM) is employed to construct a virtual entity of DT. The main contributions of this work include:

a) the innovative application of LSTM to construct the virtual entity of WTs;

b) the proposal of a criterion to define the sub-healthy state of WTs; and

c) the design of a novel intelligent system to evaluate the state of WTs and facilitate the maintenance arrangements.

The motivation for proposing the iSEMA system is to better monitor the status of WTs and to schedule the maintenance more effectively. Typically, wind farm operators perform maintenance on a WT until the system enters a period of low wind speed. If slight or mild anomalies in power generation can be identified in advance and addressed earlier, then multiple manual shutdowns may be prevented and avoided, thereby minimizing WT downtime and maximizing economic returns. The iSEMA system proposed in this study can effectively identify the "sub-healthy" state of WTs: a state where a WT's performance has already deteriorated but obvious faults have not yet manifested. The system records the monitoring process and alerts wind farm operators once any "sub-healthy" state occurs. Operators can then judiciously schedule maintenance activities accordingly.

This study focuses on WT's operating under both steady and turbulent wind conditions, covering a range of wind speeds from low to high, as typically observed in inland and offshore environments. The system is designed to account for varying wind patterns, including turbulence intensity and vertical wind shear, which are critical for accurate performance assessment.

The remainder of this article is organized as follows. Section 2 introduces the relevant methods. Section 3 demonstrates the details of the proposed system. In Section 4, experimental results are presented and analyzed. The final section provides a summary of the work.

2. Literature review of related methods

2.1. Long short-term memory

The recurrent neural network (RNN) is an important type of deep learning model and has been widely employed in many different fields. Compared with other deep learning models, the main difference is that RNNs have a powerful capability of handling time series data and extracting nonlinear features [18]. **Figure 1** shows the basic structure of an RNN which has a special delay layer that can store previous memory [19]. Although RNNs perform well with time-series data, traditional RNNs suffer from gradient vanishing and gradient explosion issues. In addition, traditional RNNs cannot keep long-term information [18]. To solve this problem, the gate mechanism [20] was introduced to form a special type of RNN, called long short-term memory (LSTM), and the inner structure is shown in **Figure 2**.

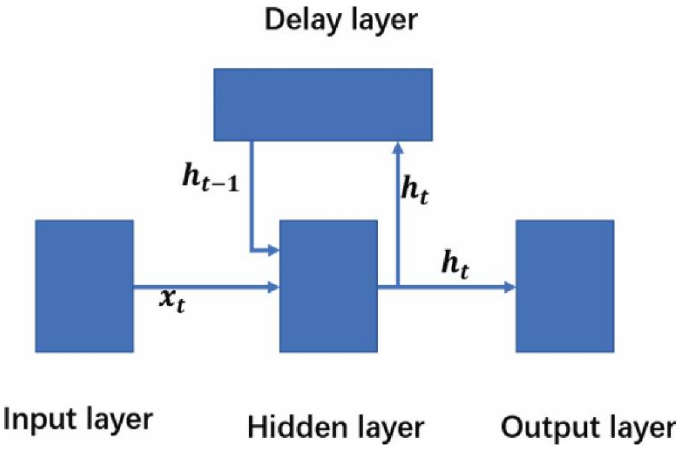

Figure 1 • The structure of recurrent neural network.

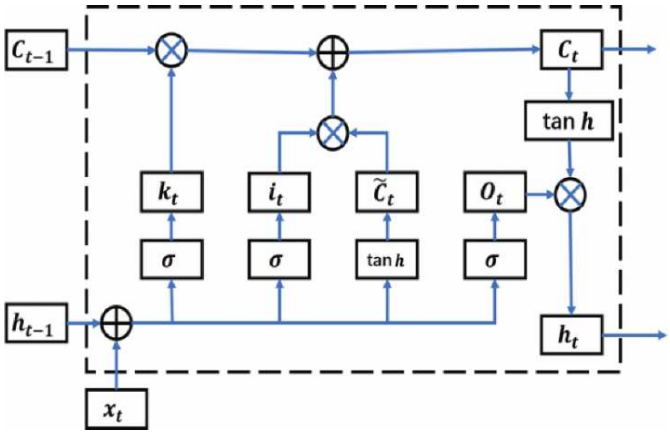

Figure 2 • The inner structure of the long short-term memory unit.

The introduction of three gates and a memory cell state C_t into the RNN structure enables LSTM to have both long-term and short-term memory; the hidden state is known as short-term memory and the cell state is known as long-term memory [21]. The following formula is used in the calculation of the LSTM unit:

$$\begin{bmatrix} c_t \\ o_t \\ i_t \\ k_t \end{bmatrix} = \begin{bmatrix} \tanh \\ \sigma \\ \sigma \\ \sigma \end{bmatrix} \left(W \begin{bmatrix} x_t \\ h_{t-1} \end{bmatrix} + b \right) \tag{1}$$

$$c_t = k_t c_{t-1} + i_t c_t \tag{2}$$

$$h_t = o_t \tanh\left(c_t\right) \tag{3}$$

where k_t, i_t, and o_t represent the forget, input gate, and output gate, respectively; x_t and h_t are the input and hidden state, respectively; c_t and c_t are the updated cell state and the candidate cell state, respectively; W is the parameter associated with input and hidden state, and b is the bias parameter vector.

LSTM has been widely used in time series data prediction, natural language processing, text recognition, and so on [22] due to its advantages of handling time series data and addressing the exploding gradient problems. This work is concerned with the description of the dynamic behaviors of WTs using various environment signals and to predict the generated power of WTs in different environments. In this article, the generated power refers to the power produced by WTs in operational scenarios under health conditions. Data used in this article, such as power output and environmental conditions, are time series in nature, and LSTM networks have been shown to outperform traditional methods in capturing such temporal patterns [23]. While traditional regression models or other machine learning models could be used for power prediction, they cannot capture the temporal dependencies present in WT data. LSTM, on the other hand, is specifically designed to model such time series data, making it a more suitable choice for predicting both short-term fluctuations and long-term performance trends.

2.2. Digital twin

DT technology represents a digital replica of a physical system that continuously updates with real-time data from the physical counterpart. The primary advantage of DTs is their ability to simulate, monitor, and predict the behavior of physical systems, thus allowing for better decision-making and optimization [3]. Since the concept of DT was proposed in 2003, its content and connotation, structure, framework, implementation, and so on have been extensively investigated and developed. Nowadays, DT encompasses not only the virtual representation of physical entities but also focuses on the exchange of data between physical entities and their virtual counterparts, as well as using the virtual entities to enhance the performance of the physical entities [4]. In recent years, DT technology has been adopted in various industries, including manufacturing, healthcare, and increasingly, renewable energy, particularly in the wind energy sector [24]. An illustration of DT is shown in **Figure 3**. A twin indicates that the behavior or the state of the physical entity and virtual entity are equal to some degree. Once a change takes place in the physical entity, the change is delivered to the virtual entity by the signals or information. Then, the virtual entity will adjust the parameters to reach equality. Similarly, once a change has happened in the virtual entity, the change is delivered to the physical entity by the feedback information; therefore, the physical entity will adjust the parameters and get better performance.

Note the structure of DT shown in **Figure 3** is not fixed; it can be adjusted or changed to meet different specific application requirements. For example, Tao et al. [25] introduced a criterion to better describe DT after analyzing 10 application areas of DT. It divided DT into five dimensions, namely physical entity, virtual model, connection, data, and service, where the virtual model consists of four sub-models (i.e., geometric model, physical model, behavioral model, and rule model). Based on the criterion proposed by Tao et al. [25], Tao et al. [26] analyzed 63 publications on manufacturing and found that only 29 of them included all four sub-models.

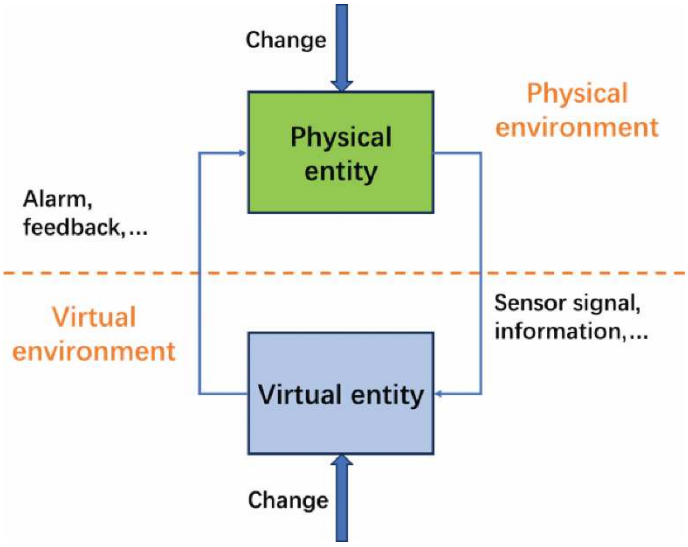

Figure 3 • An illustration of digital twin.

The application of DT technology to WTs offers several key advantages that significantly enhance the operational efficiency and reliability of WT systems including real-time monitoring, predictive maintenance, improving the reliability of WTs, extension of component service life, and improvement of operational efficiency [27, 28]. First, DTs facilitate real-time monitoring by integrating sensor data from the turbine's various components, allowing for continuous performance assessment and early detection of anomalies. This real-time insight enables timely intervention, reducing the risk of unexpected failures and improving overall WT safety. For example, in their work [29], Dinh et al. proposed an assisted condition monitoring system based on DT for a 2-MW class double-fed induction generator-based WT which showed a good performance. In one study [30], researchers used a DT-based approach to simulate the real operation condition of the WT drive train system and monitor the operation of WTs with the introduction of particle swarm optimization least squares support vector machine. The experimental results demonstrated that it can significantly enhance fault diagnosis accuracy and response speed, achieving a 99.1% success rate.

Second, predictive maintenance is another major benefit enabled by DT technology. Through the analysis of historical and real-time operational data, DTs allow for the accurate forecasting of maintenance needs, thus optimizing maintenance schedules and minimizing downtime and associated costs. In another study [31], the researchers had a detailed discussion about the distributed DT framework for predictive maintenance with a specific case study on WTs and demonstrated how the edge-fog-cloud paradigm can optimize DT implementation for predictive maintenance in WTs. Third, DTs play a crucial role in improving the reliability of WTs. By continuously updating virtual models with real-world data, they provide decision support that allows for more precise predictions of system behavior under various conditions, thereby reducing the likelihood of unplanned outages. In their [32], Wang et al. provided an overview of recent developments in the reliability analysis of offshore WT support structures, with particular emphasis on the incorporation of DT technology alongside finite element modeling. Thus, they proposed a novel DT framework that facilitates real-time monitoring and data integration, thereby enhancing the operational reliability and safety of offshore wind energy

systems. Fourth, another notable advantage is the extension of component service life, achieved by using DTs to monitor fatigue and performance degradation. This enables more efficient asset management, ensuring that WTs continue to operate effectively even as they near the end of their design life. Some researchers have discussed and proposed methods to predict the remaining useful life of WTs based on DT technology [33, 34]. They think that DT technology can track and extend the lifespan of WT components. Finally, operational efficiency is significantly enhanced through the actionable insights provided by DTs, which optimize energy production, resource allocation, and overall wind farm performance.

A WT has many different subsystems, for example, wind capture system, generator system, control system, and so on. The decrease in power generation due to the WT being in a sub-healthy state is just a superficial observation. Various faults of different subsystems can potentially contribute to this phenomenon. Therefore, despite the fact that one single DT can assess the state of the WT quite well, as will be shown in this study, it cannot provide more specific details of a fault, such as the location or the type of the fault. Due to these reasons, sub-DTs should be constructed based on different subsystems of the WT, and then these sub-DTs must be integrated into the overall DT constructed for the whole WT system. The relationship between WT and DT, together with their respective subsystems, is shown in **Figure 4**.

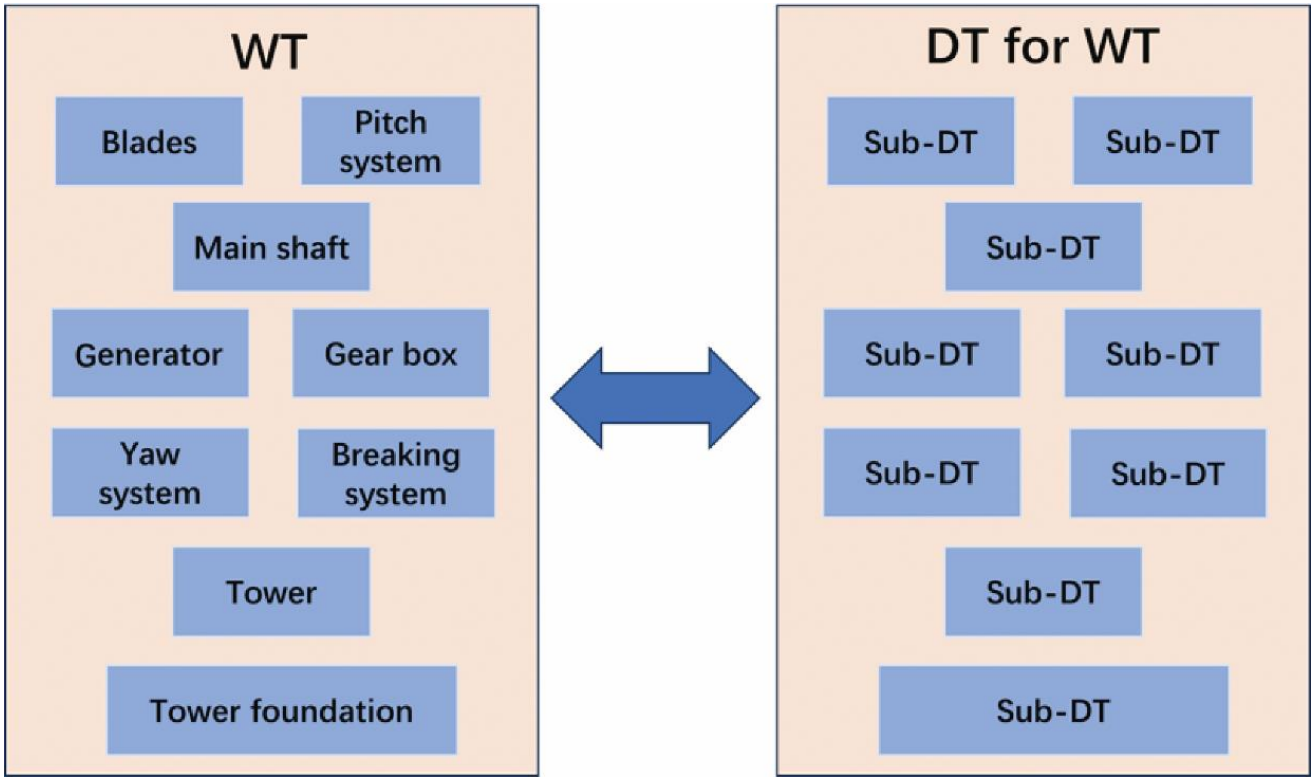

Figure 4 • The relationship between wind turbine and digital twin, together with their respective subsystems. DT, digital twin; WT, wind turbine.

3. Proposed system

The iSEMA system operates by integrating multiple sources of data, including actual measured power out and environmental signals such as wind speed, direction, air density, and so on. These signals are gathered in real time and compared with the predicted power output generated by the LSTM model. The system's decision-making is based on deviations between predicted and actual power outputs, thereby diagnosing the healthy or sub-healthy state of the WT. For example, once the power output drops below a predefined threshold (for example, 90%), the system evaluates this deviation over a series of days to determine if the WT is entering a sub-healthy state.

The structure of the proposed iSEMA system is shown in **Figure 5**, where historical data under various physical environmental conditions (e.g., wind speed, direction, air density, air pressure, and temperature) can be collected from the associated meteorological masts around WTs. Then, the data are divided into two parts, namely training data and test data. After that, the training data and test data are separately fed to the mathematical model, which is the virtual representation of WTs. In this work, the mathematical model is constructed by LSTM, because LSTM has the advantages of handling time series data and addressing the exploding of gradient problems. In addition, the criterion for determining whether a WT is in a healthy or sub-healthy condition is the difference between the actual power generated by the WT and the predicted power over a long time. Therefore, the output of this mathematical model is a prediction of sequence data, and LSTM is good at handling these sequence problems [22]. The function of this mathematical model is to describe the behavior and assess the states of the WT by predicting the generated power of the WT under different environments. More details of the proposed network model including the settings of the associated hyper-parameters (e.g., the number of hidden units and the optimization method used) are shown in Section 4.

Once the mathematical model is constructed and well trained, collected online (in-time) data can then be fed into the model to assess the states of the WT. By comparing the predicted power and actual power, the proposed iSEMA system can distinguish

the state of the WT, which is either normal (healthy) or abnormal (sub-healthy). The system will send an alarm and information to operators if the WT is in an abnormal state. Follow-up maintenance can then be arranged based on the feedback signals.

To the best of our knowledge, there is no specific universal criterion to clearly define, characterize, and discriminate the sub-healthy state of WTs. Typically, the sub-healthy state of a WT refers to an operational condition in which the WT is still functioning but has deviated from its optimal performance for a long period. In this state, WT exhibits signs of performance degradation or emerging anomalies that indicate potential risks, though these signs have not yet resulted in a complete failure or necessitated immediate shutdown. The introduction of the "sub-healthy" state concept is pivotal for preventing severe failures in WTs. Traditionally, WTs are categorized as either "healthy" or "faulty." However, this binary classification overlooks the early signs of performance degradation. By defining a sub-healthy state, the iSEMA system allows for more proactive maintenance scheduling, thereby reducing unplanned downtime and extending the lifespan of critical WT components. If early warnings are sent to the WT monitoring and management center, then the concerned team can address these warnings during regular maintenance work instead of waiting until the sub-healthy state develops or leads to more serious faults. This will significantly improve the efficiency of the WT and reduce any potential downtime.

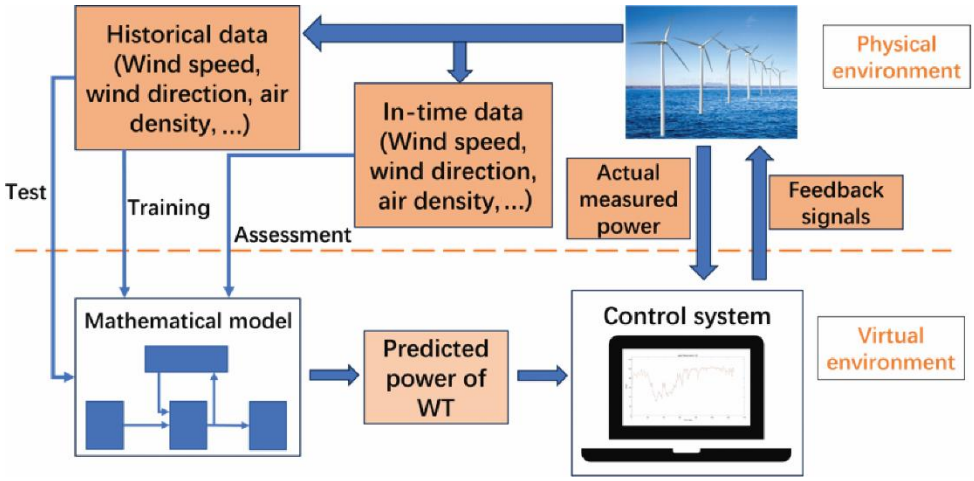

Figure 5 • The structure of the proposed intelligent state evaluation and maintenance arrangement system. WT, wind turbine.

The conceptual scope of sub-healthy state of WT includes the following:

(1) Performance deviation: The operational parameters of WT, such as power output (used in this article), rotational speed, vibration levels, or temperature, deviate from their designed optimal ranges, though the deviation is not severe enough to cause a breakdown.

(2) Early warning signs: The sub-healthy state is characterized by the presence of early-stage anomalies that hint the onset of potential failures or accelerated wear, indicating that WT is at an increased risk of future malfunction if left unaddressed.

(3) Need for monitoring and maintenance: While the WT can continue operating in the sub-healthy state, this condition needs close monitoring and preemptive maintenance to prevent further deterioration or failure.

(4) Short-term operability: Despite being in a sub-healthy condition, the WT remains operational without significant immediate impacts on its power generation capacity. However, continued operation in this state over time may accelerate wear and lead to major faults or system breakdowns.

The exclusions of sub-healthy state of WT are as follows:

(1) Critical failure or shutdown: Once the WT reaches a state where it requires immediate shutdown or repair, it is no longer in the sub-healthy state but in a failure or fault state.

(2) Optimal health: In the healthy state, the WT operates within all specified design parameters, without any signs of performance degradation or potential faults.

In this article, the sub-healthy state of a WT is defined from two aspects, namely the dimension of power and the dimension of time. To better define the sub-healthy state of the WT, it is necessary to introduce three relevant quantities first as follows:

(1) CP: A criterion for determining whether the WT is in a sub-healthy state or a healthy state, which is typically represented as a certain percentage (CP).

(2) Dmax: The maximum number of consecutive occurrences of sub-healthy days (Dmax) in historical data determined by the system.

(3) PSDP: The proportion of accumulated sub-healthy data points (PSDP) to the total number of data points in each day.

With the above quantities, the sub-healthy state of a WT can be described by the following three steps:

(1) When the power of a data point at a specific moment is lower than a CP of the predicted generated power, then that data point is seen as a sub-healthy data point.

(2) If the proportion of accumulated sub-healthy data points to the total number of data points (PSDP) is larger than a specific value within 1 day, then that day is seen as a sub-healthy day.

(3) If the situation continuously remains for Dmax+1 days, the WT is seen as in a sub-healthy state.

In the iSEMA system, the time scale of 1 day (24 hours) is used as the measurement unit for the indicator Dmax. Note that the total sub-healthy time determined by the system is fixed once the historical data were given. A smaller measurement unit (e.g., less than 24 hours), such as 12 hours, would not be a good choice because such a unit can increase the value of Dmax.

For different types of WTs, the values of CP, Dmax, and PSDP are usually different; however, typically, the value of CP should be specified or determined in advance based on a priori knowledge or empirical experience. In this work, CP is chosen to be 90%; such a threshold is adjustable for specific requirements and applications. There is not a standard rule that can be used to choose the value of CP; in general, the value should be less than 100% and it is not suggested to set CP to a value less than 70%. For a high CP value (e.g., exceeding 90%), the iSEMA system may not accurately determine the state of WTs. Furthermore, in practical scenarios, the actual power output of WTs may occasionally be slightly lower than the generated power, and usually this is not considered a faulty state. Therefore, a CP value that is very close to 100% is impractical. On the other hand, opting for a relatively low CP value, such as 50%, would imply that the system will not work until the actual power falls below 50% of the generated power. Again, this is an impractical or ineffective option. Once the value of CP is given, the proposed iSEMA system can automatically obtain the value of PSDP and Dmax and provide the information to operators in time. For convenience, it is necessary to introduce another indicator, called the ratio of adjusted power to the actual measured power (RoAP2MP) which is used to manually adjust the power of WTs during simulations to evaluate a sub-healthy state behavior. For convenience, the adjusted power refers to the power changed based on RoAP2MP and the measured power. Once the parameters and settings of the iSEMA system are determined, its performance can then be tested using the proposed models and methods. By changing the value of RoAP2MP, different states of WTs can be simulated. For example, by setting the value of RoAP2MP to 70%, simulations can be conducted to test if the iSEMA system can distinguish the WT is in a sub-healthy state. The algorithm of the diagnosis system is shown in **Table 1**.

Table 1 • The algorithm of diagnosis system

Step 1	Divide the historical data into three parts: training data, validation data, and test data, in the ratio of 6:2:2.
Step 2	Give the value of CP and set the value of RoAP2MP to CP+1%.
Step 3	Increase the value of PSDP from 50% to 100%, increasing by 5% each time to obtain the corresponding Dmax on training data.
Step 4	Obtain all the values of Dmax that are less than 10 along with their corresponding PSDP.
Step 5	Apply all the Dmax and corresponding PSDP on validation data and obtain the best pair of Dmax and PSDP that takes the shortest time to distinguish the sub-healthy state.
Step 6	Apply the best Dmax and PSDP on test data to test if it works.

CP, certain percentage; RoAP2MP, ratio of adjusted power to the actual measured power; PSDP, proportion of accumulated sub-healthy data points.

Based on the above descriptions and discussion of defined quantities, it is clear that, in the iSEMA system, the sub-healthy state is determined using these quantities, such as CP, PSDP, and Dmax, which quantify deviations from optimal performance over time. CP evaluates the WT's power output efficiency, with values below 90% indicating that WT may be in a sub-healthy state. If the power output continues to be below CP and exceeds PSDP for a continuous day in statistics, then that day is considered a sub-healthy day. Note that Dmax is the maximum number of consecutive occurrences of sub-healthy days in historical data determined by the system. Since LSTM's prediction of power output is not completely accurate, a normal day may be mistaken for a sub-healthy day. By introducing Dmax, it reduces the misjudgment of the WT's sub-healthy state caused by inaccurate LSTM predictions to a certain extent. Together, these metrics, namely CP, PSDP, and Dmax, provide a detailed understanding of the turbine's operational health and are critical for predicting maintenance needs. This allows the system to capture long-term trends in power output degradation, which might otherwise go unnoticed in traditional fault detection systems. By incorporating these parameters, the iSEMA system can provide early warnings of suboptimal performance.

4. Experiments and results

4.1. Experiments and data description

The experimental design was guided by several key assumptions. First, we assumed that, despite differences in environmental conditions, the fundamental operational patterns of WTs remain similar. This assumption allowed us to use the same model architecture for both inland and offshore WTs. Second, we hypothesized that the LSTM model, with its LSTM capabilities, would effectively capture the nonlinear and time-varying dynamics of WT operations. The choice of adaptive moment estimation (Adam) as the optimization algorithm was based on its superior experimental performance as confirmed by its lowest root mean square error (RMSE) in comparison with other optimizers. Finally, considering that the WT lifecycle extends far beyond four years, it is assumed that the data of actual measured power output (inland and offshore power data) are the same as that of the generated power in Section 4. That is to say, the WT is assumed in a healthy state for the first four years of its lifespan.

The selection of variables, including wind speed, wind direction, air density, turbulence intensity, and so on, was based on their direct impact on the power generation and mechanical stress of WTs. These environmental factors are crucial for assessing WT performance and predicting potential faults. The LSTM model was chosen for its abilities to handle time series data and capture long-term dependencies, which are essential for modeling WT

behaviors. Furthermore, the 6:2:2 split of data into training, validation, and test sets was carefully selected to ensure that sufficient data were available for training while retaining enough for unbiased validation and testing.

To validate the effectiveness and robustness of the iSEMA system, the experiments were designed to cover a variety of environmental conditions and WT types, including offshore and inland WTs. This approach ensures that the system can generalize well across different operational scenarios. The primary goal of the experiments was to assess the system's ability to diagnose the healthy and sub-healthy states of WTs under diverse conditions. The decision to include multiple types of WTs was motivated by the need to confirm that the iSEMA system could be generalized and applied to a broad range of real-world scenarios.

This section provides two case studies: one for offshore wind power data analysis and modeling, and the other focusing on the data related to inland WTs. The work by Ding [35] provides the data for both cases, which are measured and collected during the first four years of the turbine's operations. The data were recorded every 10 minutes from the WTs; environment signals, such as wind speed, wind direction, air density, turbulence intensity, and so on, were collected from the around meteorological masts. For each case study, data were collected from the same type of WTs but with different locations. In this study, data from one WT are employed to construct the iSEMA system, and data from other WTs (of the same type but installed at different location) are employed to evaluate the performance of the proposed system. To illustrate the daily variations of WTs, each sample comprises 144 data points.

The public data used in this article are collected from real practice WTs and associated meteorological masts. The coordinates of WTs and meteorological masts in the data are added with a constant by the real coordinates for protecting their true geographic information. The authenticity ensures that the data are representative of the WT operational behaviors we aim to model, making them suitable for training and testing the iSEMA system. The data have been used and validated in studies because, on the webpage of this dataset, it can be found that the data have been viewed more than 2,000 times and downloaded more than 500 times.

In this study, data from different sources were used without standardization. The decision not to standardize the data was made to preserve the original characteristics of the signals, which could be essential for capturing the nuanced behavior of WTs under varying environmental conditions. Although no explicit standardization was performed, the data used in this study share common characteristics. All power outputs were collected from operational WTs using similar sensor configurations and all environment information was collected from the closest meteorological masts, ensuring a level of consistency across different data sources. These shared attributes allowed us to analyze the data collectively without the need for further normalization, as the data exhibited common temporal and structural patterns.

4.2. Experiments on offshore data

4.2.1. Design of the virtual model

For the offshore case, there are two WTs, namely WT3 and WT4. Data from WT3 are employed to construct the proposed iSEMA system and data from WT4 are employed to test the performance of the designed system. As described in Section 3, LSTM neural networks are used to build the virtual model, whose input signals are wind speed, wind direction, air density, humidity, and turbulence intensity. Wind speed is the primary driver of power output, while wind direction affects the alignment and efficiency of the WT blades. Air density plays a key role in determining the energy available in the wind, with variations affecting power generation efficiency. Humidity affects the aerodynamic properties of the air and can contribute to material degradation, particularly in offshore environments. Finally, turbulence intensity significantly influences mechanical stress and fatigue, making it critical for predicting long-term turbine health. The unrolled structure of proposed LSTM networks is shown in **Figure 6**, where x^t, c^t, and h^t are the input data, memory data, and hidden data at time step t, respectively. Because the length of each sample is 144, the total number of time steps is 144.

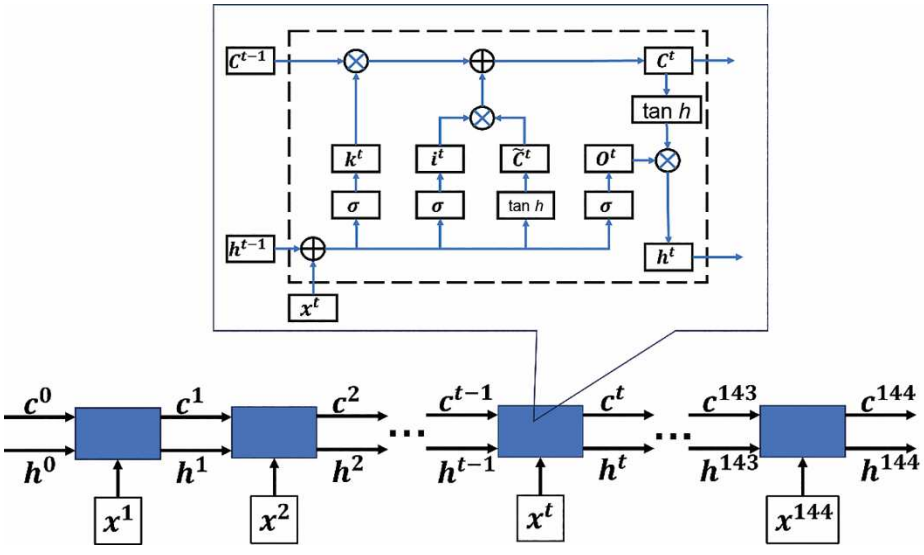

Figure 6 • The unrolled structure of proposed long short-term memory networks.

To obtain an LSTM network model with best performance, a two-step scheme is performed to choose the most suitable optimization algorithm and determine the best number of hidden units of the LSTM networks. In step 1, the optimization method is chosen one by one from stochastic gradient descent with momentum (SGDM), root mean square propagation (RMSProp), and Adam, with other parameters being kept constant. SGDM was selected for initial model optimization due to its ability to accelerate convergence by incorporating a momentum term. This helps the model navigate areas of high curvature more efficiently and avoid local minima, making it suitable for training complex models like LSTM where gradient instability is a potential challenge. RMSProp was evaluated due to its ability to adaptively adjust the learning rate for each parameter, which is particularly useful in time series data like WT performance. This method helps smooth out the learning process by controlling the update step for parameters that exhibit different levels of variability, thus enhancing model stability. Adam was ultimately chosen for its superior performance in balancing convergence speed, and stability. By combining the advantages of SGDM (momentum) and RMSProp (adaptive learning rate), Adam consistently achieved lower RMSE in our experiments, making it the optimal choice for fine-tuning the LSTM-based iSEMA system.

Figure 7 demonstrates the RMSE of LSTM under different optimization methods for 10 trials. It can be seen that the LSTM model trained with Adam performs best in terms of RMSE, with an average value of 18.71. While SGDM and RMSProp offered specific benefits in terms of momentum and adaptive learning rates, Adam provided the best overall performance, allowing for faster convergence and lower prediction error, thus becoming the preferred optimizer for this study.

Based on the experimental results of step 1, the Adam optimization method is used for further model training. Thus, in step 2, Adam is used to train different LSTM networks with different number of hidden units, ranging from 50 to 250 with an increase of 50 each time. For each of the cases (with different number of hidden units), a total of 10 experiments were carried out and the results are shown in **Figure 8**. From the experimental results, when the number of hidden units equals to 150, the LSTM network shows the best performance in terms of the average RMSE value, which is 16.25. Note that among all the trained models, the LSTM network model with 150 hidden units shows the best performance, with an RMSE value of 8.85 in the last trial. Therefore, this LSTM model is selected as the virtual representation of WT3.

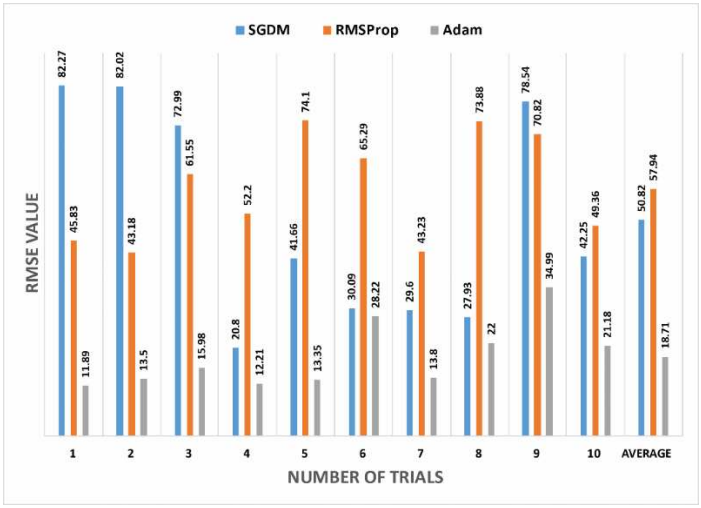

Figure 7 • The root mean square error of long short-term memory under different optimization methods. Adam, adaptive moment estimation; RMSProp, root mean square propagation; SGDM, stochastic gradient descent with momentum.

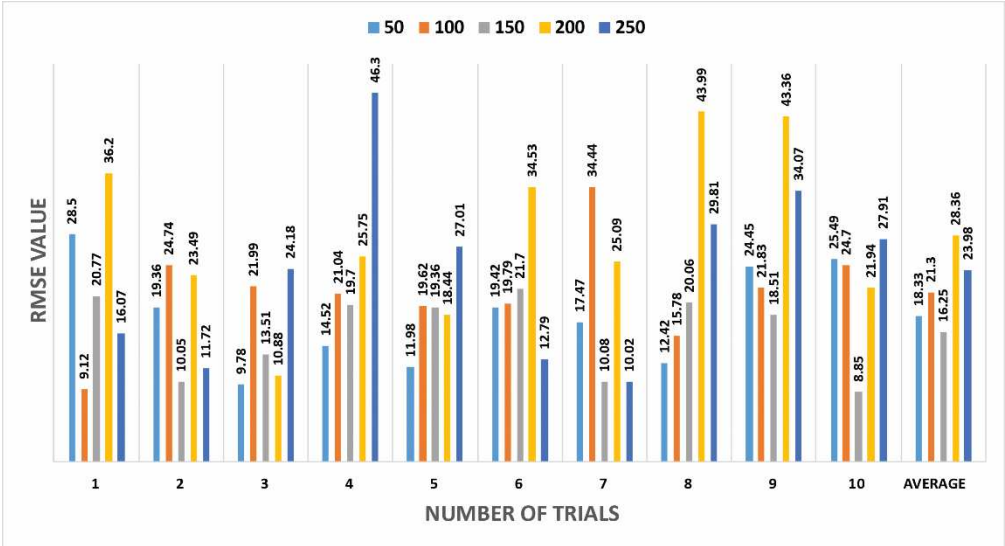

Figure 8 • The root mean square error of long short-term memory for different number of hidden units.

The distribution of the RMSE values of final selected LSTM model on the test data is shown in **Figure 9**. From the RMSE distribution of LSTM for the test data, it can be seen that the distribution of RMSE resembles a normal distribution. **Figure 10** shows a comparison between the actual measured power and the corresponding model predictions on the offshore test dataset within 1 day. In most cases, the selected LSTM model has a good performance, but at certain times, the predictions are not accurate. For example, from **Figure 10**, it can be observed that the virtual model (LSTM networks) can predict the power generation very well. However, it can be noted that for the first around 55 data points, the actual values are higher than the predicted values, whereas for data points from around 105 to 125, the actual values are lower than the predicted values.

To avoid the influence of imprecise predictions on WT state assessment and diagnosis, two indicators, namely PSDP and Dmax, defined in the previous section, are introduced to the proposed iSEMA system. The local indicator PSDP, which is related to the accumulated sub-healthy data points, is insensitive to the bias in model prediction of the generated power in a short time as long as the prediction errors are small. For example, if PSDP is defined as 90% for the proposed system, then any proportion of misjudged data points less than this value can be avoided. By introducing the global indicator Dmax, the proposed system can address some extreme scenarios. For example, if the value of PSDP is small and the proportion of misjudged data points is larger than PSDP, then the WT state on that day would be classified as in a sub-healthy state. Note that the value of Dmax is associated with the maximum number of consecutive occurrences of sub-healthy days in historical data. In this situation, Dmax would become larger and allows the proposed iSEMA system to address such an extreme scenario.

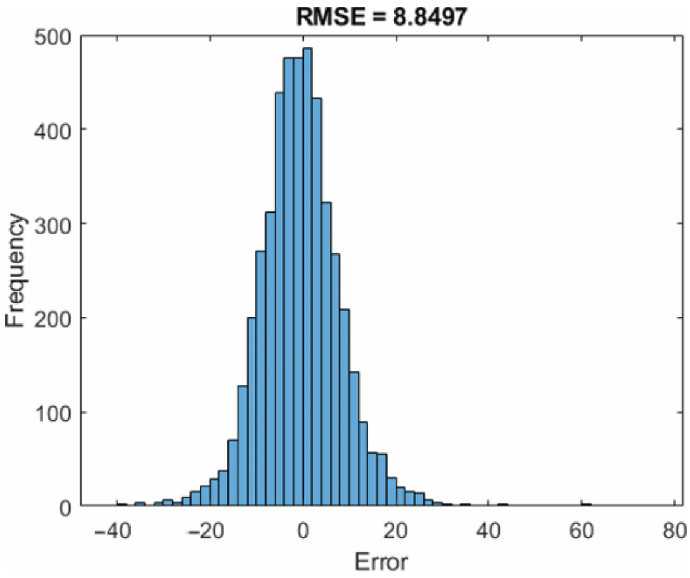

Figure 9 • The root mean square error distribution of long short-term memory in the test data. RMSE, root mean square error.

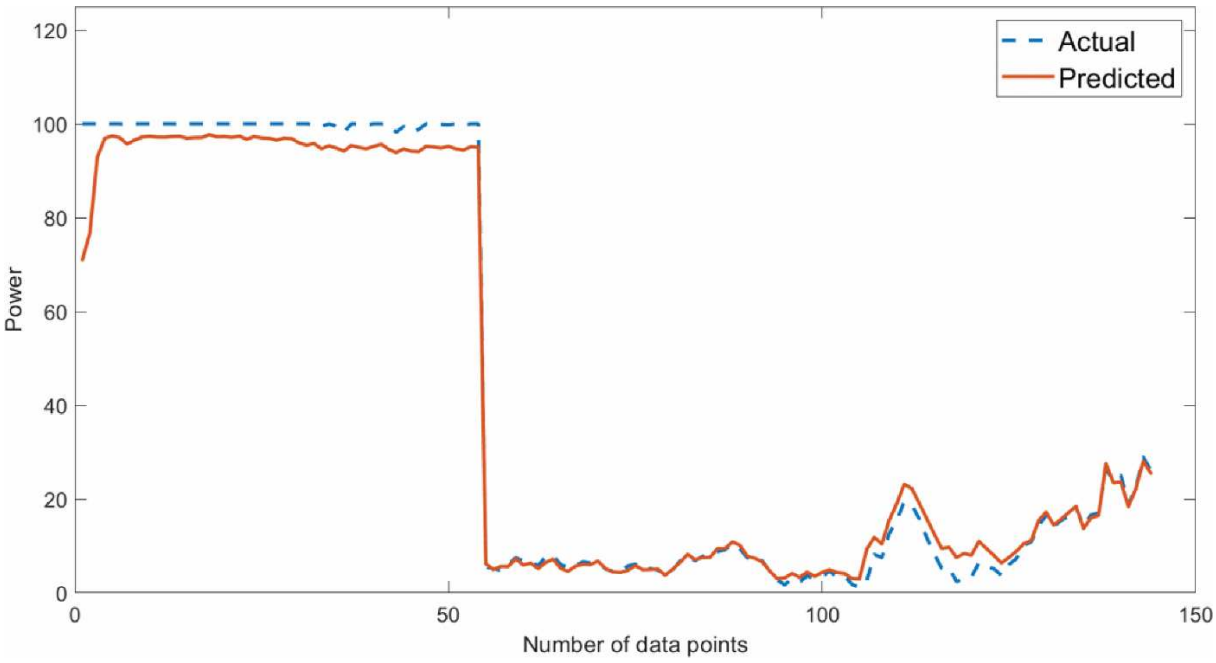

Figure 10 • A comparison between the actual measured power and the predicted generated power in the offshore test dataset.

4.2.2. Selection of indicators for the diagnosis system

Once the LSTM model is well trained, the data are redivided into three parts: training, validation, and test data in the ratio of 6:2:2 to determine the best value of indicators for the diagnosis system. The sample length is 144 and the numbers of samples for training, validation, and test data are 471, 157, and 157, respectively. In this article, the CP is set to 90%, indicating that if the value of power data point at a specific moment is lower than 90% of the predicted value, then that data point is treated to be a sub-healthy point. As mentioned earlier, the global indicator Dmax is the maximum number of consecutive occurrences of sub-healthy days determined by the system, and PSDP is the local indicator related to the proportion of accumulated sub-healthy data points to the total number of data points in each day. Typically, the value of Dmax decreases with the increase of RoAP2MP when the value of PSDP is constant. To illustrate this, an experiment is carried out on the training data, with the following settings: the value of PSDP is set to be constant (50%); the value of RoAP2MP changes from 85% to 93% with an increase of 1% each time. The model was then simulated by considering different states of WT1. The resulting values of Dmax are shown in **Table 2**.

The results in **Table 2** demonstrate that the value of Dmax decreases with the increase of RoAP2MP when the value of PSDP is constant. In addition, when the value of RoAP2MP exceeds 90%, the value of Dmax keeps constant. If the parameter CP is set to be 90%, then when the proposed DT model iSEMA is used to simulate the WTs, all samples whose RoAP2MP is less than 90% will be treated as sub-healthy samples, resulting in a large value of Dmax. When WT is healthy, samples with RoAP2MPbeing larger than 90% will be seen as healthy samples. However, due to the errors in the LSTM model, some healthy samples may be misclassified as sub-healthy, resulting in a relatively small value of Dmax.

To make the diagnosis system robust, reliable, and effective, the following two considerations are put together in the iSEMA system design. First, the diagnosis system should be able to effectively avoid misclassifying a healthy state as a sub-healthy state. Second, the system should be able to detect a sub-healthy state of WTs as quickly as possible. In doing so, when selecting the two parameters, Dmax and PSDP, the resolution capability for situations where RoAP2MP is larger than CP (i.e., RoAP2MP is larger than 90%) is considered first. Furthermore, based on the results reported in **Table 2**, when RoAP2MP is larger than CP, Dmax remains unchanged. Therefore, the selection of Dmax and PSDP should be carried out under the premise of RoAP2MP being equal to CP+1%, as shown in **Table 1** (step 2). In this way, most misdiagnoses of misclassifying a healthy state as a sub-healthy state can be avoided. For cases where RoAP2MP is larger than CP, but Dmax decreases instead of remains unchanged, the premise of RoAP2MP being equal to CP+1% still works. This is because if a relatively larger Dmax is chosen as the criterion for determining sub-healthy states, then the cases with a smaller Dmax will be classified as healthy states correctly. For example, if RoAP2MP is set to 90% and assume Dmax is 5, meaning that the WT is healthy, but it is on the verge of entering a sub-healthy state, then the maximum number of consecutive occurrences of sub-healthy days determined by the system is 5. Note that, if the situation of sub-healthy days persists for Dmax+1 (i.e., 6) consecutive days, the WT is seen as in sub-healthy state. When RoAP2MP is larger than 90%, the value of Dmax would be equal to or less than 5 which is smaller than 6. Therefore, a healthy WT state misjudged as sub-healthy is avoided. Based on the above discussions and the procedure given in **Table 1**, simulation experiments are carried out with the following settings: (1) the values of power are set to 91% of the actual measured power for all the samples on the training data, and (2) PSDP increases from 50% to 100%. The change of Dmax is shown in **Table 3**.

Table 2 • The changes of Dmax with different RoAP2MP and proportion of accumulated sub-healthy data points being fixed at 50% for the offshore WT3 training data (unit: day)

RoAP2MP	85%	86%	87%	88%	89%	90%	91%	92%	93%
Dmax	89	84	46	28	27	17	17	17	17

WT, wind turbine; RoAP2MP, ratio of adjusted power to the actual measured power.

Table 3 • The change of Dmax with different proportion of accumulated sub-healthy data points and RoAP2MP being fixed at 91% for the offshore WT3 training data (unit: day)

PSDP	50%	55%	60%	65%	70%	75%	80%	85%	90%	95%	100%
Dmax	17	17	17	15	15	12	12	11	7	4	2

RoAP2MP, ratio of adjusted power to the actual measured power; PSDP, proportion of accumulated sub-healthy data points; WT, wind turbine.

The results in **Table 3** demonstrate that when RoAP2MP is set to 91%, a larger PSDP value leads to a smaller Dmax. Note that if the situation of sub-healthy day continuously remains for Dmax+1 days as described in Section 3, then the WT is seen as in a sub-healthy state. Clearly, the magnitude of Dmax directly influences the time required for determining the sub-healthy state of a WT. A prolonged evaluation period, in turn, may adversely impact the power generation or even WT shutdown, thereby incurring economic loss. The best values of Dmax and PSDP may be chosen from the last three pairs in **Table 3**, based on which Dmax can be chosen as 7, 4, or 2. It is recommended that the value of Dmax should be smaller than 10. By choosing the last four pairs of Dmax and PSDP from **Table 3**, experiments are carried out on the validation data of WT3. When the value of PSDP changes from 85% to 100%, the condition cases are marked as A, B, C, and D, respectively. The experimental results are recorded in **Table 4**. Note that a WT will usually enter into a sub-healthy state at a certain point after an extended period of normal operation, thereby resulting in a decrease in power generation. To sufficiently cover such realistic scenarios in the simulation experiments, the values of the WTs' power are adjusted based on RoAP2MP for part of the validation samples.

In **Table 4**, *H* means the state of WT3 is diagnosed as healthy by the designed iSEMA system. According to the results reported in **Table 4**, when the WT is healthy and the adjusted power maintains at or above 90% of actual measured power, the system can make the correct judgment for all the four condition cases. When RoAP2MP is within the range of 84%–89%, it means the WT is in a sub-healthy state; the diagnosis system cannot correctly determine the WT state for any of the four condition cases. When the adjusted power decreases to 83% of actual measured power, only the condition Case C (Dmax is 4 and PSDP is 95%) can make the correct judgment. It takes 6 days from the point where the adjusted power consistently falls to or below 83% of actual measured power, until then the system confirms that the WT is in a sub-healthy state. Although the system performs best for condition Case C among all the four condition cases, it still has an error when RoAP2MP is within the range of 84%–89%. Compared with condition Case C, it usually requires a longer time for assessment or has a relatively larger error for other cases. Therefore, this work selects condition Case C, the most difficult tasks among the four, as a benchmark to show the performance of the proposed method. To test if condition Case C is suitable for WT3, experiments are conducted first on the test data and results are recorded in **Table 5**.

Experimental results in the test data demonstrate that when the WT is healthy and the adjusted power can be maintained at 90% of actual measured power or above, the diagnosis system can make the correct judgment. When the WT is in a sub-healthy state and the adjusted power decreases to 84% of actual measured power or lower, the system can determine that the WT is sub-healthy, but it takes 6 days to make a correct judgment, from the point where the adjusted power consistently falls to or below 84% of actual measured power until the system confirms that the WT is in a sub-healthy state.

The results in **Table 6** demonstrate that the proposed system has a relatively worse performance for WT4 in comparison with that for WT3. This may be attributed to the operating and environment conditions. When WT4 is healthy, the system can make correct judgment. When the WT is sub-healthy and the adjusted power decreases to 86% of actual measured power, it takes 8 days for the system to determine the sub-healthy state. The number of days required for determination is increased, but the error decreases.

To further validate the feasibility of the proposed system, experiments are conducted on the data collected from WT4. Note that WT4 is the same type as WT3; both are offshore WTs installed in different locations. With the same model and experimental settings as for WT3, the results for WT4 are shown in **Table 6.**

Table 4 • Days required to determine sub-healthy state of WT3 for different RoAP2MP for the offshore validation dataset (unit: day)

Cases	RoAP2MP									
	75%	80%	81%	82%	83%	84%	85%	89%	90%	95%
A	22	22	22	23	H	H	H	H	H	H
B	7	20	20	H	H	H	H	H	H	H
C	4	5	5	6	6	H	H	H	H	H
D	15	H	H	H	H	H	H	H	H	H

RoAP2MP, ratio of adjusted power to the actual measured power; H, healthy; WT, wind turbine.

Table 5 • Days required to distinguish sub-healthy state of WT3 for different RoAP2MP under condition Case C in the offshore test dataset

RoAP2MP	75%	80%	81%	82%	83%	84%	85%	89%	90%	95%
Days	4	6	6	6	6	6	H	H	H	H

RoAP2MP, ratio of adjusted power to the actual measured power; H, healthy; WT, wind turbine.

Table 6 • Days required to distinguish sub-healthy state of WT4 for different RoAP2MP under condition Case C

RoAP2MP	75%	80%	81%	82%	85%	86%	87%	89%	90%	95%
Days	8	8	8	8	8	8	H	H	H	H

RoAP2MP, ratio of adjusted power to the actual measured power; H, healthy; WT, wind turbine.

After the evaluation of WTs, if the WT is in a sub-healthy state, the proposed iSEMA system can send an alert (as shown in **Figure 11**) to the associated staff (operators or workers). In addition, the proposed iSEMA system can provide an in-time comparison chart between the actual measured power and the predicted generated power as shown in **Figure 12**. By making use of the alerts and in-time comparison chart provided by the system, operators can proactively schedule maintenance work during periodic maintenance, and address potential issues and significantly improve the efficiency of WT.

```
The wind turbine is now under sub-healthy sate and it starts from:
   2007-06-23 02:50:00
```

Figure 11 • The alert provided by the system.

4.3. Experiments on inland data

For inland data, there are also two WTs, namely WT1 and WT2. Data from WT1 are employed to construct the iSEMA system, while data from WT2 are employed to test the feasibility of the proposed system. Wind speed, wind direction, air density, turbulence intensity, and vertical wind shear were collected as input to construct the LSTM model, whose structure is shown in **Figure 6**. The difference in variables between the inland and offshore data arises from the inherent environmental differences between the two locations. Inland WTs are more influenced by factors such as humidity and turbulence intensity due to complex terrain and atmospheric conditions. In contrast, offshore WTs experience more consistent wind patterns, making variables like turbulence intensity and vertical wind shear more critical. These differences are naturally present in the raw data and reflect the distinct operational challenges faced by WTs in each environment. To construct the LSTM model, the priority is to

define the parameters of the LSTM networks by applying the same method described in Section 4.2.1. The following two-step scheme is employed: (1) choosing the best optimization method from SGDM, RMSProp, and Adam, and (2) determining the best number of hidden units. Finally, the number of hidden units is set to 150 and the optimization method used is Adam. To demonstrate the performance of the LSTM model, a comparison between the actual measured power from inland WT1 and the corresponding model predictions is shown in **Figure 13**.

Once the LSTM model is well trained, it can then be used for simulation studies. In this work, the experiments are designed as follows: (1) splitting the inland data into three parts: training data, validation data, and test data in the ratio of 6:2:2; (2) setting the value of CP to 90%; (3) obtaining the possible values of PSDP and Dmax in the training data; and (4) determining the best pair of PSDP and Dmax in the validation data. The experimental results on the training data are recorded in **Table 7**.

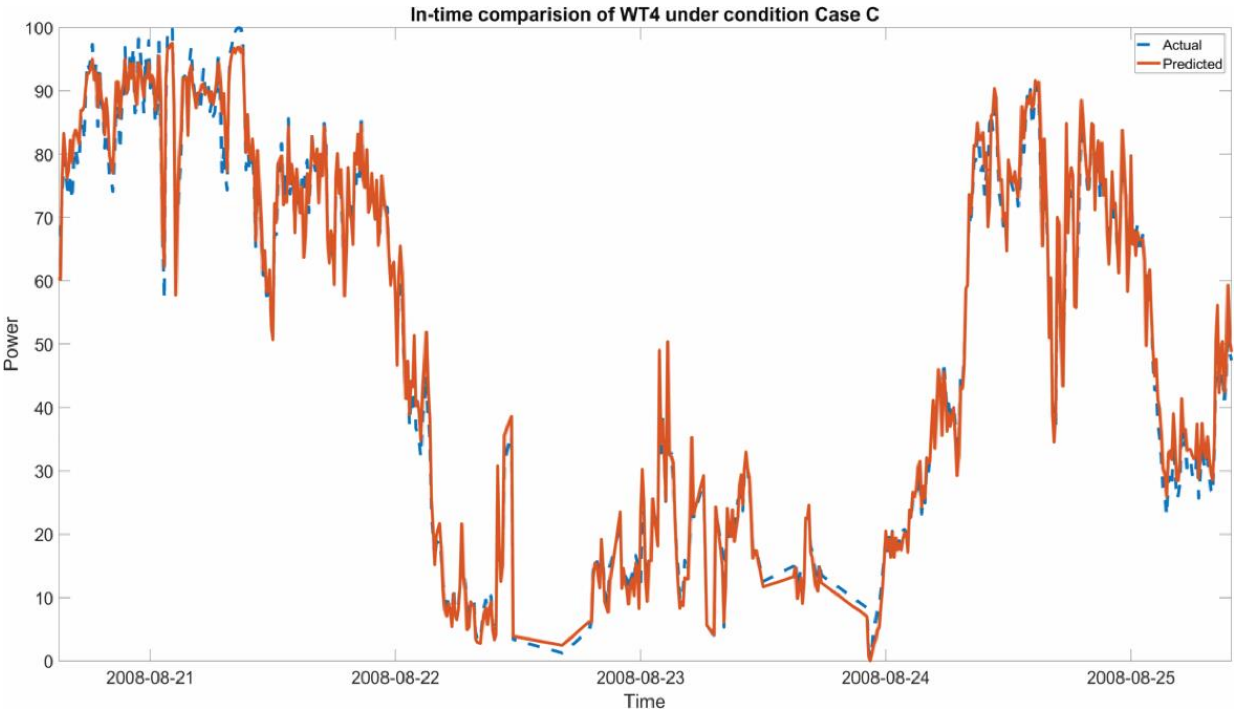

Figure 12 • The in-time comparison chart produced by the intelligent state evaluation and maintenance arrangement system of offshore WT4 under condition Case C. WT, wind turbine.

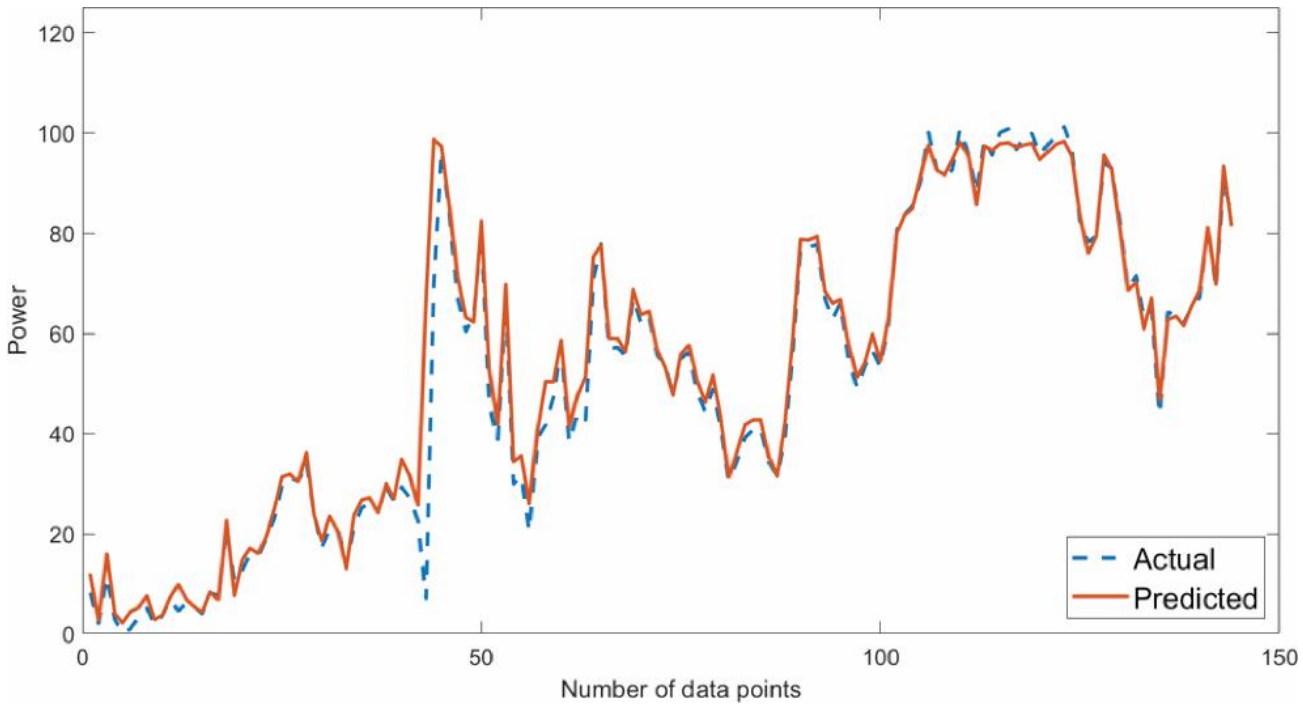

Figure 13 • A comparison between the actual measured power and the predicted generated power for the inland test dataset.

Table 7 • The change of Dmax with different proportion of accumulated sub-healthy data points and RoAP2MP being fixed at 91% in the inland WT1 training data

PSDP	50%	55%	60%	65%	70%	75%	80%	85%	90%	95%	100%
Dmax	77	32	29	20	20	20	5	4	2	2	0

RoAP2MP, ratio of adjusted power to the actual measured power; PSDP, proportion of accumulated sub-healthy data points; WT, wind turbine.

To enable the system to distinguish the state of WTs quickly, the value of Dmax should not be too large; it is suggested to be smaller than 10. Here, the last five pairs of indicators in **Table 7** are used as a reference to determine the value of PSDP. By using the last five values of PSDP in **Table 7** and choosing 10 different values of RoAP2MP, numerical experiments were carried out on the data for WT1. **Table 8** shows some results of the assessment of the state of WT1 under different conditions in the validation data.

Table 8 • Days required to determine sub-healthy state of WT1 for different RoAP2MP in the inland validation dataset (unit: day)

PSDP	RoAP2MP									
	75%	80%	81%	84%	85%	86%	87%	89%	90%	95%
80%	5	5	5	7	7	7	H	H	H	H
85%	4	4	4	6	6	H	H	H	H	H
90%	2	4	4	4	4	6	H	H	H	H
95%	2	4	4	4	6	H	H	H	H	H
100%	1	3	5	5	H	H	H	H	H	H

RoAP2MP, ratio of adjusted power to the actual measured power; H, healthy; PSDP, proportion of accumulated sub-healthy data points; WT, wind turbine.

When the adjusted power maintains at or above 90% of actual measured power, the system can make the correct judgment for all the five PSDP conditions (80%–100%). Note that when RoAP2MP is below 90%, the WT state is defined as sub-healthy. From **Table 8**, it can be seen that when RoAP2MP is between 87% and 89%, meaning that the WT is in a sub-healthy sate, the diagnostic system incorrectly classifies them as a health state. When the adjusted power decreases to 86% of actual measured power, the system makes the correct judgment for the first and third cases of five PSDP conditions (80% and 90%, respectively), but fails to make correct judgment for other cases. When the adjusted power drops to 84% of actual measured power, the system makes correct judgment for all the five cases. It can be noted from **Table 8** that the diagnostic system performs relatively better for the third case (PSDP = 90%) than for the other cases. Therefore, the third case is used in further simulation study. Experiments are carried out on test data, and the results are recorded in **Table 9**.

Experimental results on the test data demonstrate that when the WT is healthy and the adjusted power maintains at 93% of actual measured power or above, the system can make the correct judgment. However, when the WT is actually healthy and the adjusted power is within the range of 90%–92% of actual measured power, the system classifies the WT state as in a sub-healthy. Such errors may be explained as follows: In **Table 1**, step 3 is to find the best indicators (Dmax and PSDP) on the training data to avoid misclassifying a healthy state as a sub-healthy state. However, due to the uncertainty and changes in the internal and external working environment of the WTs, the distribution of test data may not be exactly the same as that of the training data. Therefore, the selected indicators based on the training data may not best fit the test data. For example, if the best value of Dmax should be 10, and PSDP should be 90%, but the selected Dmax is 6 and PSDP is 80% based on the training data, then errors may occur when the trained diagnostic system is applied to a test dataset. As a consequence, it may misclassify a healthy state as a sub-healthy state. When the adjusted power decreases to or below 89% of actual measured power, the system works better on the test data: it can correctly determine the WT state. It takes 2 days to make the correct judgment.

To further validate the feasibility of the proposed system, experiments are conducted on the data collected from WT2. Note that WT2 is the same type as WT1; both are inland WT but installed in different locations. With the same model and experimental settings as for WT1, the results on the whole data for WT2 are shown in **Table 10**.

Table 9 • Days required to distinguish sub-healthy state of WT1 for different RoAP2MP under the third condition case on the test dataset

RoAP2MP	75%	80%	85%	88%	89%	90%	91%	92%	93%	95%
Days	2	2	2	2	2	2	2	2	H	H

RoAP2MP, ratio of adjusted power to the actual measured power; H, healthy; WT, wind turbine.

Table 10 • Days required to distinguish sub-healthy state for different RoAP2MP on the whole data of WT2 under the third condition case

RoAP2MP	75%	80%	81%	82%	83%	84%	85%	89%	90%	95%
Days	2	2	2	6	9	9	H	H	H	H

RoAP2MP, ratio of adjusted power to the actual measured power; H, healthy; WT, wind turbine.

The results demonstrate that the proposed system showed a relatively worse performance on WT2 compared to WT1. The reason may be attributed to the change of operating conditions and work environment. When WT2 is healthy, the system can make correct judgment. When the WT is in sub-healthy and the adjusted power decreases to 84% of actual measured power, it takes 9 days for the system to determine the sub-healthy state. The number of days required for determining the state is increased, and the range of error becomes larger. Overall, the proposed iSEMA system, trained with the data of WT1, works well for WT2. An advantage of the iSEMA system is that there is no need to retrain the LSTM model or re-select the values of indicators if the WTs are the same type.

4.4. Discussion

Using the proposed iSEMA system, it is possible to evaluate and predict the state of WTs by modeling and analyzing historical data of WTs. The selection of Dmax and PSDP is important for achieving quick and reliable diagnosis results as the two parameters have significant influence on the time required to distinguish the state of WTs. The proposed iSEMA system can distinguish the sub-healthy state of WTs quickly once the actual measured power of a WT decreases to a certain degree. Experimental results demonstrate that when the actual measured power maintained at or above 90% of the predicted generated power, the system can diagnose the healthy state correctly. However, when the actual measured power is set in the rough range from 85% to 89% of the predicted generated power, the diagnosis accuracy of iSEMA system is reduced. It was observed that, if the selected indicators are not good enough, misjudgment may occur as shown in **Table 9**.

In addition, the model trained using the data of one WT can also be applied to other WTs of the same type, installed at different locations. This is important for improving the overall evaluation and maintenance efficiency for large-scale wind farms, as models trained based on data of some WTs can be directly applied to other WTs without making major changes or adjustments to the pre-trained models deep learning models.

5. Conclusions

In this work, the concept and definition of the sub-healthy state of WTs are expounded by introducing three parameters: CP, PSDP, and Dmax (Section 3). A novel iSEMA system designed based on DT technique is then proposed. The system can automatically evaluate the state of WTs and provide information useful for monitoring the state of WTs and scheduling maintenance more effectively. Thus, the efficiency of WTs can be highly improved.

The iSEMA system's performance was evaluated using data from both inland and offshore WTs. Each dataset was split using the 6:2:2 method. Metrics like RMSE and the number of days required to diagnose a sub-healthy state were used to measure the model performance. The iSEMA system is highly adaptable and can be applied to various WT types and environmental conditions without retraining the model for each new site. Once the iSEMA system is trained based on data collected from one specific WT, it can be directly applied to other same type WTs in different locations. This flexibility comes from the fact that the LSTM-based model learns underlying patterns between WT behavior and environment information, which are transferrable between similar machines. The system is designed for ease of integration into existing maintenance workflows, enabling operators to preemptively address potential issues before they escalate into major faults.

A deficiency of the proposed iSEMA system is that when the measured power of WTs is within the rough range of 85%–89% of the predicted generated power, the model system may not always distinguish the state of WTs accurately. Furthermore, if the distribution of the test data is significantly different from the training data (which frequently occurs in real problem solving), then the selected indicators may not be good enough; as a consequence, misjudgment of the WT state can occasionally occur. Therefore, it is essential to regularly adjust and update the associated parameters to maintain good performance of the system.

It is worth mentioning that the iSEMA system cannot provide specific information on the types or locations of WT faults. In future, more experiments on sub-DT, involving key specific components of WT, will be carried out by incorporating different sub-DT systems into the iSEMA system, to enable the system to provide more specific details of faults and therefore significantly improve the accuracy of the iSEMA system.

Acknowledgments

The authors acknowledge that this work was supported in part by both the Royal Society International Exchanges 2022 Cost Share (NSFC) (Ref. IEC\NSFC\223266) and EPSRC (Ref. EP/H00453X/1).

Funding

The work was supported in part by both the Royal Society International Exchanges 2022 Cost Share (NSFC) (Ref. IEC\NSFC\223266) and EPSRC (Ref. EP/H00453X/1).

Author contributions

Conceptualization, G.W. and H.L.W.; methodology, G.W. and H.L.W.; software, G.W.; validation, G.W., H.L.W. and Z.H.L.;

formal analysis, G.W.; investigation, G.W.; resources, G.W. and H.L.W.; data curation, G.W.; writing—original draft preparation, G.W. and H.L.W.; writing—review and editing, G.W., H.L.W. and Z.H.L.; visualization, G.W.; supervision, H.L.W.; project administration, G.W. and H.L.W.; funding acquisition, H.L.W. and Z.H.L. All authors have read and agreed to the published version of the manuscript.

Conflict of interest

The authors declare no conflict of interest.

Data availability statement

Data supporting these findings are available within the article, at https://doi.org/10.20935/AcadEng7391, or upon request.

Institutional review board statement

Not applicable.

Informed consent statement

Not applicable.

Additional information

Received: 2024-07-15

Accepted: 2024-10-14

Published: 2024-10-28

Academia Engineering papers should be cited as *Academia Engineering 2024*, ISSN 2994-7065, https://doi.org/10.20935/AcadEng7391. The journal's official abbreviation is *Acad. Engg*.

Publisher's note

Academia.edu Journals stays neutral with regard to jurisdictional claims in published maps and institutional affiliations. All claims expressed in this article are solely those of the authors and do not necessarily represent those of their affiliated organizations, or those of the publisher, the editors, and the reviewers. Any product that may be evaluated in this article, or claim that may be made by its manufacturer, is not guaranteed or endorsed by the publisher.

Copyright

References

1. Rahman A, Farrok O, Haque MM. Environmental impact of renewable energy source based electrical power plants: solar, wind, hydroelectric, biomass, geothermal, tidal, ocean, and osmotic. Renew Sustain Energy Rev. 2022;161:112279. doi: 10.1016/j.rser.2022.112279
2. Gang LI, Ying QI, Yinqiang LI, Jianfu Z, Lihui Z. Research progress on fault diagnosis and state prediction of wind turbine. Autom Electr Power Syst. 2021;45(4):180–91. doi: 10.7500/AEPS20200301002
3. Grieves M. Digital twin: manufacturing excellence through virtual factory replication. White Paper. 2014;1:1–7.
4. Jones D, Snider C, Nassehi A, Yon J, Hicks B. Characterising the digital twin: a systematic literature review. CIRP J Manuf Sci Technol. 2020;29:36–52. doi: 10.1016/j.cirpj.2020.02.002
5. Semeraro C, Olabi AG, Aljaghoub H, Alami AH, Al Radi M, Dassisti M, et al. Digital twin application in energy storage: trends and challenges. J Energy Storage. 2023;58(15):106347. doi: 10.1016/j.est.2022.106347
6. He B, Bai, KJ. Digital twin-based sustainable intelligent manufacturing: a review. Adv Manuf. 2021;9(1):1–21. doi: 10.1007/s40436-020-00302-5
7. Shahat E, Hyun CT, Yeom C. City digital twin potentials: a review and research agenda. Sustainability. 2021;13(6):3386. doi: 10.3390/su13063386
8. Wang Y, Sun W, Liu L, Wang B, Bao S, Jiang R. Fault diagnosis of wind turbine planetary gear based on a digital twin. Appl Sci. 2023;13(8):4776. doi: 10.3390/app13084776
9. Kim C, Dinh MC, Sung HJ, Kim KH, Choi JH, Graber L, et al. Design, implementation, and evaluation of an output prediction model of the 10 mw floating offshore wind turbine for a digital twin. Energies. 2022;15(17):6329. doi: 10.3390/en15176329
10. Xie X, Yang Z, Wu W, Zhang L, Wang X, Zeng G, et al. Fault diagnosis method for bearing based on digital twin. Math Probl Eng. 2022;2022:2982746. doi: 10.1155/2022/2982746
11. Guo Y, Guo LZ, Billings SA, Wei HL. Ultra-orthogonal forward regression algorithms for the identification of non-linear dynamic systems. Neurocomputing. 2016;173:715–23. doi: 10.1016/j.neucom.2015.08.022
12. Li Y, Wei HL, Billings SA, Liao XF. Time-varying linear and nonlinear parametric model for granger causality analysis. Phys Rev E. 2012;85(4):1. doi: 10.1103/PhysRevE.85.049908
13. Wei HL, Billings SA, Balikhin MA. Wavelet based non-parametric narx models for nonlinear input-output system identification. Int J Syst Sci. 2006;37(15):1089–96. doi: 10.1080/00207720600903011
14. Pandit R, Infield D, Santos M. Accounting for environmental conditions in data-driven wind turbine power models. IEEE Trans Sustain Energy. 2023;14:168–77. doi: 10.1109/TSTE.2022.3204453
15. Lin Z, Cevasco D, Collu M. A methodology to develop reduced-order models to support the operation and maintenance of offshore wind turbines. Appl Energy. 2020;259:114228. doi: 10.1016/j.apenergy.2019.114228
16. Liu ZH, Wei HL, Li XH, Liu K, Zhong QC. Global identification of electrical and mechanical parameters in

PMSM drive based on dynamic self-learning PSO. IEEE Trans Power Electron. 2018;33(12):10858–71. doi: 10.1109/tpel.2018.2801331

17. Liu ZH, Wei HL, Zhong QC, Liu K, Li XH. GPU implementation of DPSO-RE algorithm for parameters identification of surface PMSM considering VSI nonlinearity. IEEE J Emerg Sel Top Power Electron. 2017;5(3):1334–45. doi: 10.1109/jestpe.2017.2690688
18. Zhu J, Jiang Q, Shen Y, Qian C, Xu F, Zhu Q. Application of recurrent neural network to mechanical fault diagnosis: a review. 2022;36:527–42. J Mech Sci Technol. doi: 10.1007/s12206-022-0102-1
19. Zhao R, Yan R, Chen Z, Mao K, Wang P, Gao RX. Deep learning and its applications to machine health monitoring. Mech Syst Signal Process. 2019;115:213–37. doi: 10.1016/j.ymssp.2018.05.050
20. Hochreiter S, Schmidhuber J. Long short-term memory. Neural Comput. 1997;9(8):1735–80. doi: 10.1162/neco.1997.9.8.1735
21. Liu ZH, Meng XD, Wei HL, Chen L, Lu BL, Wang ZH, et al. A regularized lstm method for predicting remaining useful life of rolling bearings. Int J Autom Comput. 2021;18(4):581–93. doi: 10.1007/s11633-020-1276-6
22. Van Houdt G, Mosquera C, Napoles G. A review on the long short-term memory model. Artif Intell Rev. 2020;53(8):5929–55. doi: 10.1007/s10462-020-09838-1
23. Lei P, Ma F, Zhu C, Li T. Lstm short-term wind power prediction method based on data preprocessing and variational modal decomposition for soft sensors. Sensors. 2024;24:2521. doi: 10.3390/s24082521
24. Kritzinger W, Karner M, Traar G, Henjes J, Sihn W. Digital twin in manufacturing: a categorical literature review and classification. IFAC PapersOnline. 2018;51:1016–22. doi: 10.1016/j.ifacol.2018.08.474
25. Tao F, Liu W, Zhang M, Hu TL, Qi Q, Zhang H, et al. Five-dimension digital twin model and its ten applications. Comput Integr Manuf Syst. 2019;25(1):1–18. doi: 10.13196/j.cims.2019.01.001
26. Tao F, Xiao B, Qi QL, Cheng JF, Ji P. Digital twin modeling. J Manuf Syst. 2022;64:372–89. doi: 10.1016/j.jmsy. 2022.06.015
27. Chen B, Liu K, Yu T, Li R. Enhancing reliability in floating offshore wind turbines through digital twin technology: a comprehensive review. Energies. 2024;17:1964. doi: 10.3390/en17081964
28. Yang C, Jia J, He K, Xue L, Jiang C, Liu S, et al. Comprehensive analysis and evaluation of the operation and maintenance of offshore wind power systems: a survey. Energies. 2023;16:5562. doi: 10.3390/en16145562
29. Dinh MC, Ngo MT, Kim C, Lee SJ, Yu IK, Park M. Implementation of digital twin-assisted condition monitoring and fault diagnosis for wind turbines. In 2023 12th International Conference on Renewable Energy Research and Applications, ICRERA; 2023. p. 146–50. doi: 10.1109/ICRERA59003.2023.10269370
30. Liu H, Sun W, Bao S, Xiao L, Jiang L. Research on key technology of wind turbine drive train fault diagnosis system based on digital twin. Appl Sci. 2024;14:5991. doi: 10.3390/app14145991
31. Abdullahi I, Longo S, Samie M. Towards a distributed digital twin framework for predictive maintenance in industrial internet of things (IIOT). Sensors. 2024;24:2663. doi: 10.3390/s24082663
32. Wang M, Wang C, Hnydiuk-Stefan A, Feng S, Atilla I, Li Z. Recent progress on reliability analysis of offshore wind turbine support structures considering digital twin solutions. Ocean Eng. 2021;232:109168. doi: 10.1016/j.oceaneng.2021.109168
33. Pacheco-Blazquez R, Garcia-Espinosa J, Di Capua D, Sanchez A. A digital twin for assessing the remaining useful life of offshore wind turbine structures. J Mar Sci Eng. 2024;12:573. doi: 10.3390/jmse12040573
34. Lee SJ, Kim C, Yu IK, Ngo MT, Dinh MC, Park M. Recent progress and performance analysis on durability evaluation and remaining useful life prediction technology development for the life extension of wind turbines in korea. In 2023 12th International Conference on Renewable Energy Research and Applications, ICRERA; 2023. p. 339–43. doi: 10.1109/ICRERA59003.2023.10269432
35. Ding Y. Data science for wind energy. 1st ed. New York: Chapman and Hall/CRC; 2019. p. 1–424.